

# Axion DM detection using shift current

Genta Osaki (Utokyo)

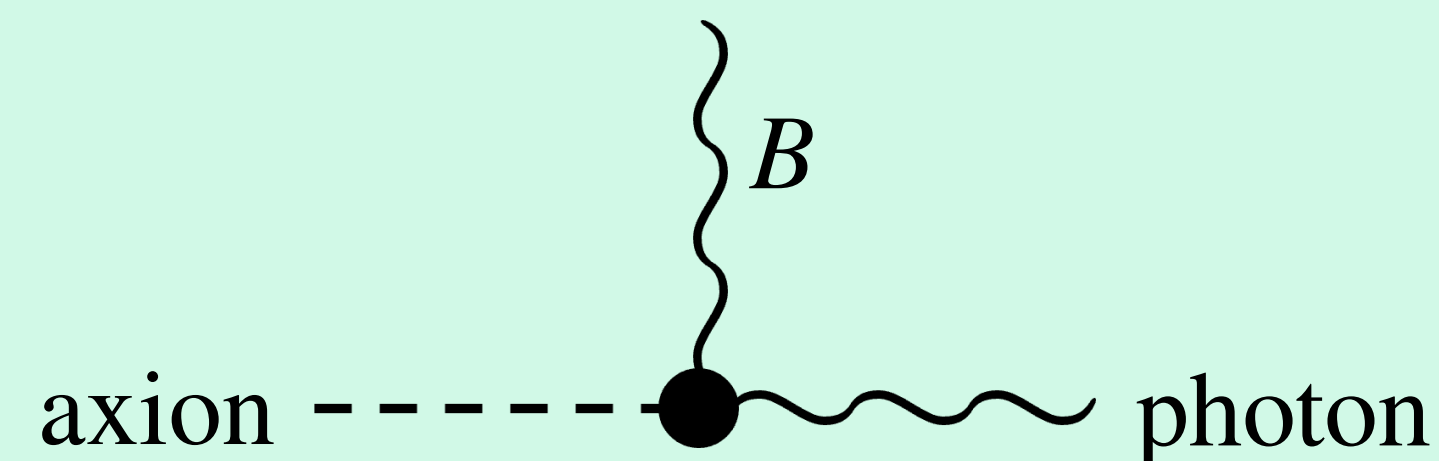
Based on the work: 2505.17007 in collaboration with Dan Kondo,  
Takahiro Morimoto, and Thanaporn Sichanugrist

# Today's topic

## Axion

Dark matter candidate

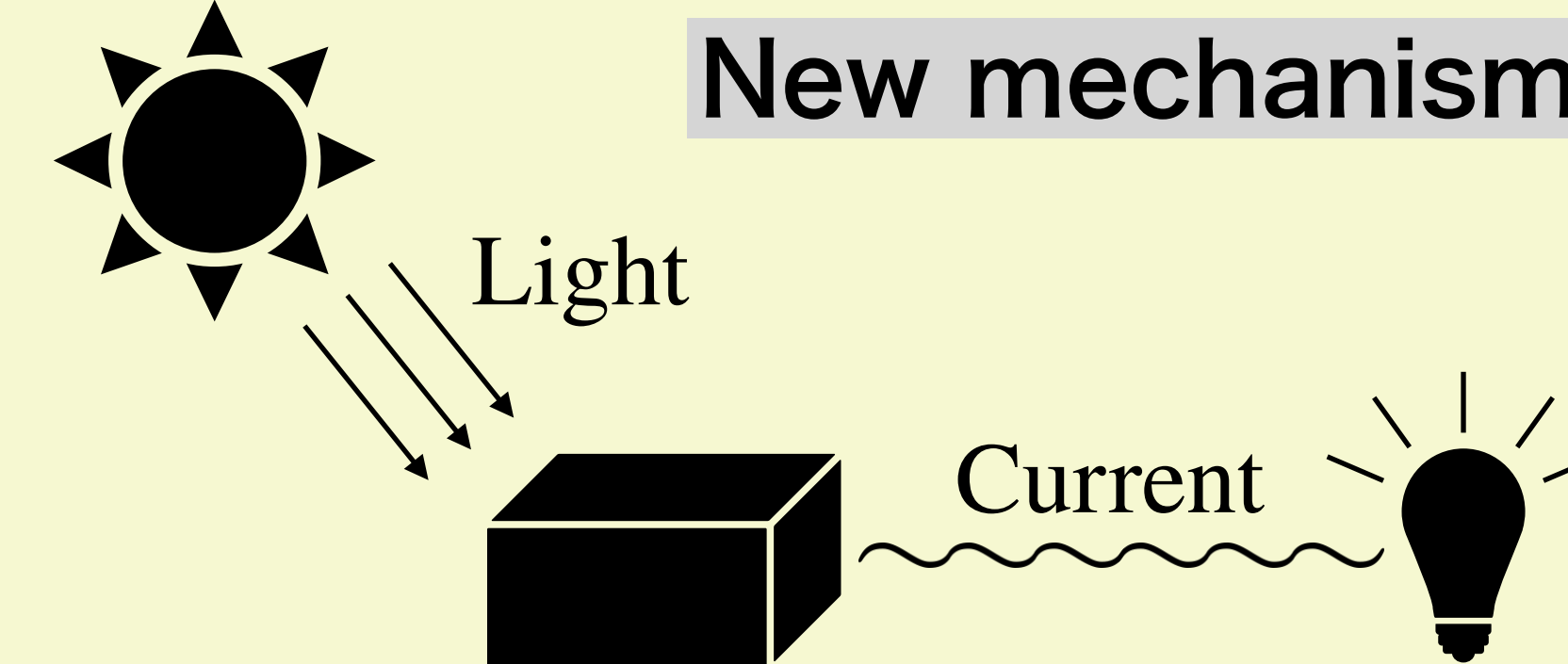
Axion-photon coupling



## Shift current

Light-induced current

New mechanism!



Our idea: Axion DM  $\rightarrow$  photon  $\rightarrow$  shift current

# Outline

- What is the shift current?
- Method to detect the axion-induced shift current

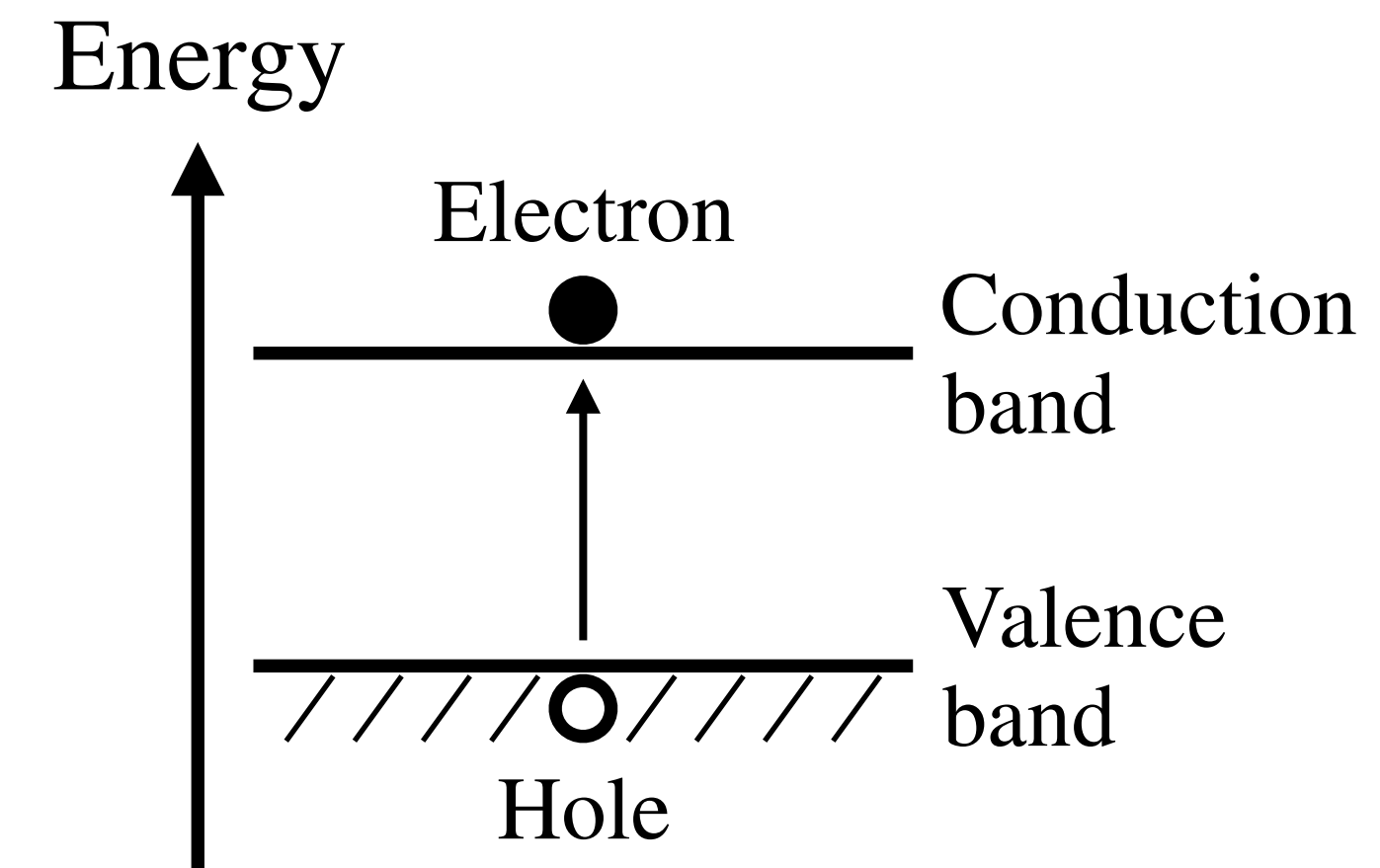
# Outline

- **What is the shift current?**
- Method to detect the axion-induced shift current

# Light-induced current

## Usual semiconductor junctions

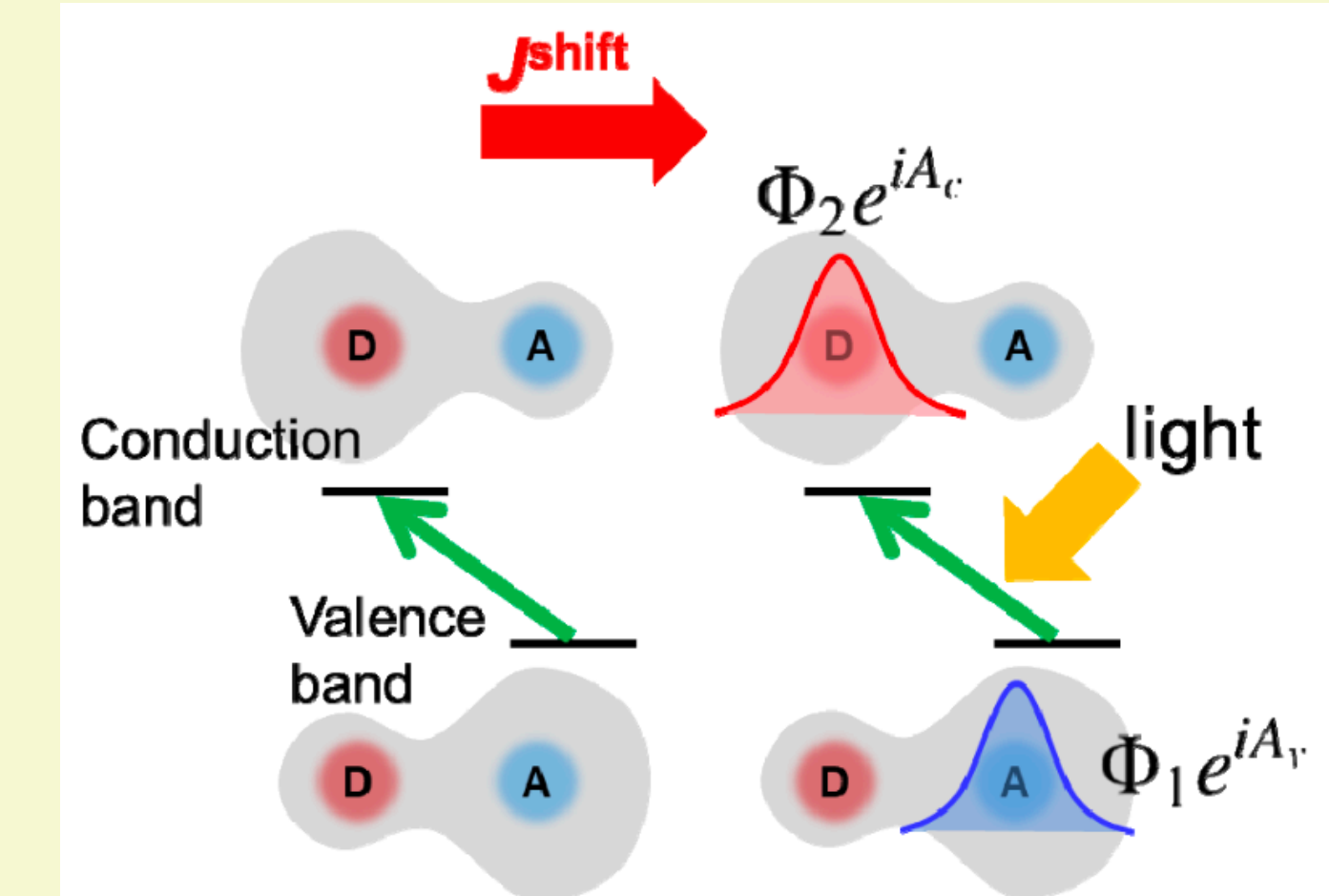
- Light creates electron-hole pairs.
- The p-n junction allows spatial separation of electron-hole pairs.



<https://www.yomiuri.co.jp/national/20240403-OYT1T50042/>

## Shift current

- Occurs in the inversion-broken materials.
- It arises from spatial shift of the electron wave function during state transitions.





記事

約 3,140 件 (0.05 秒)

プロフィール

マ-

期間指定なし

2025 年以降

2024 年以降

2021 年以降

期間を指定...

2011 — 2020

検索

Year	Papers
— 1960	25
1961 — 1970	26
1971 — 1980	63
1981 — 1990	107
1991 — 2000	344
2001 — 2010	913
2011 — 2020	3140
2021 —	3000

← Discovered around 1960

## Exciting topic recently!!

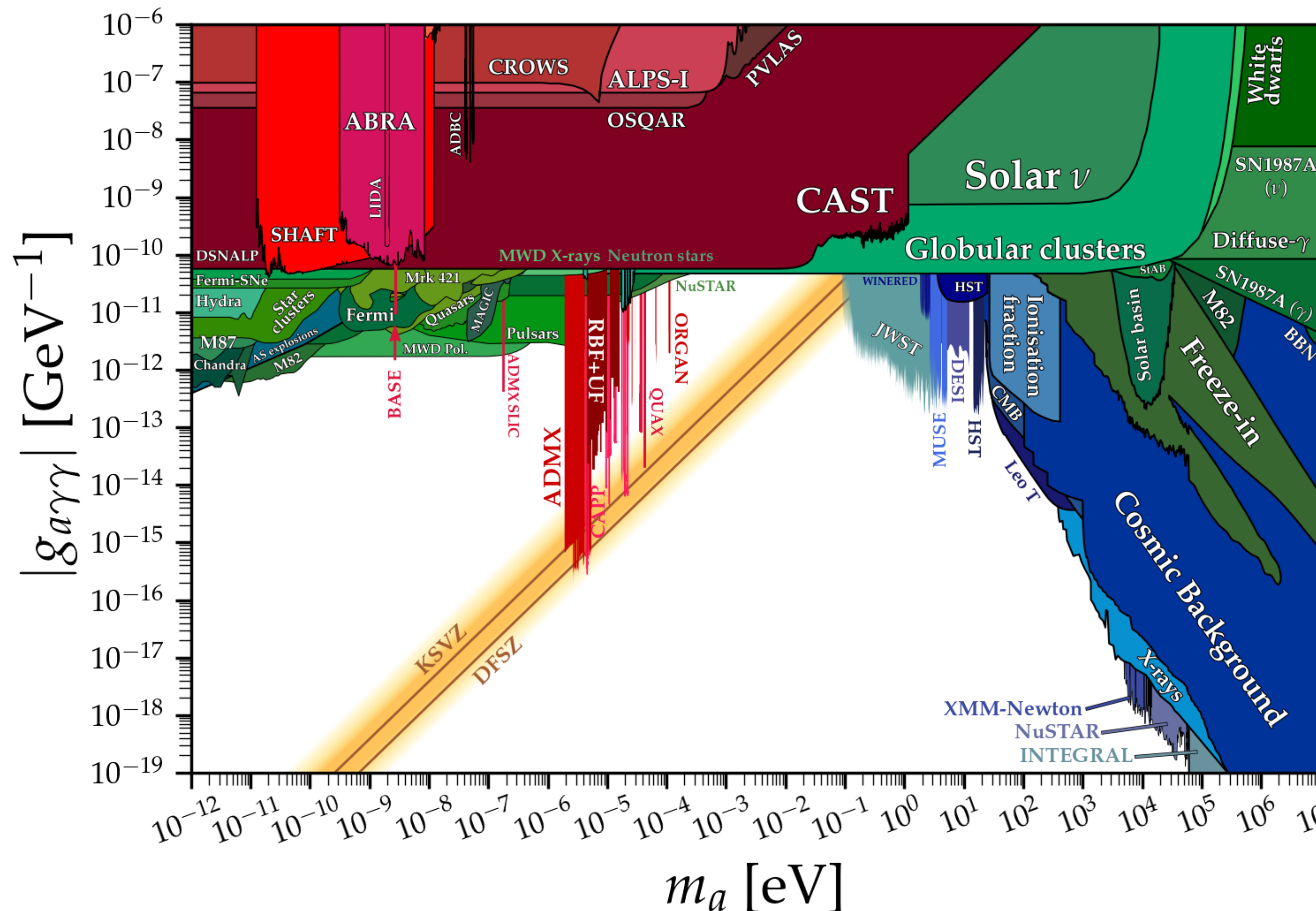
Search for materials with high efficiency

Application for new photo devices

← Theoretically well understood  
(by first principle calculation)

S. M. Young and A. M. Rappe, Phys. Rev. Lett. 109, 116601 (2012).

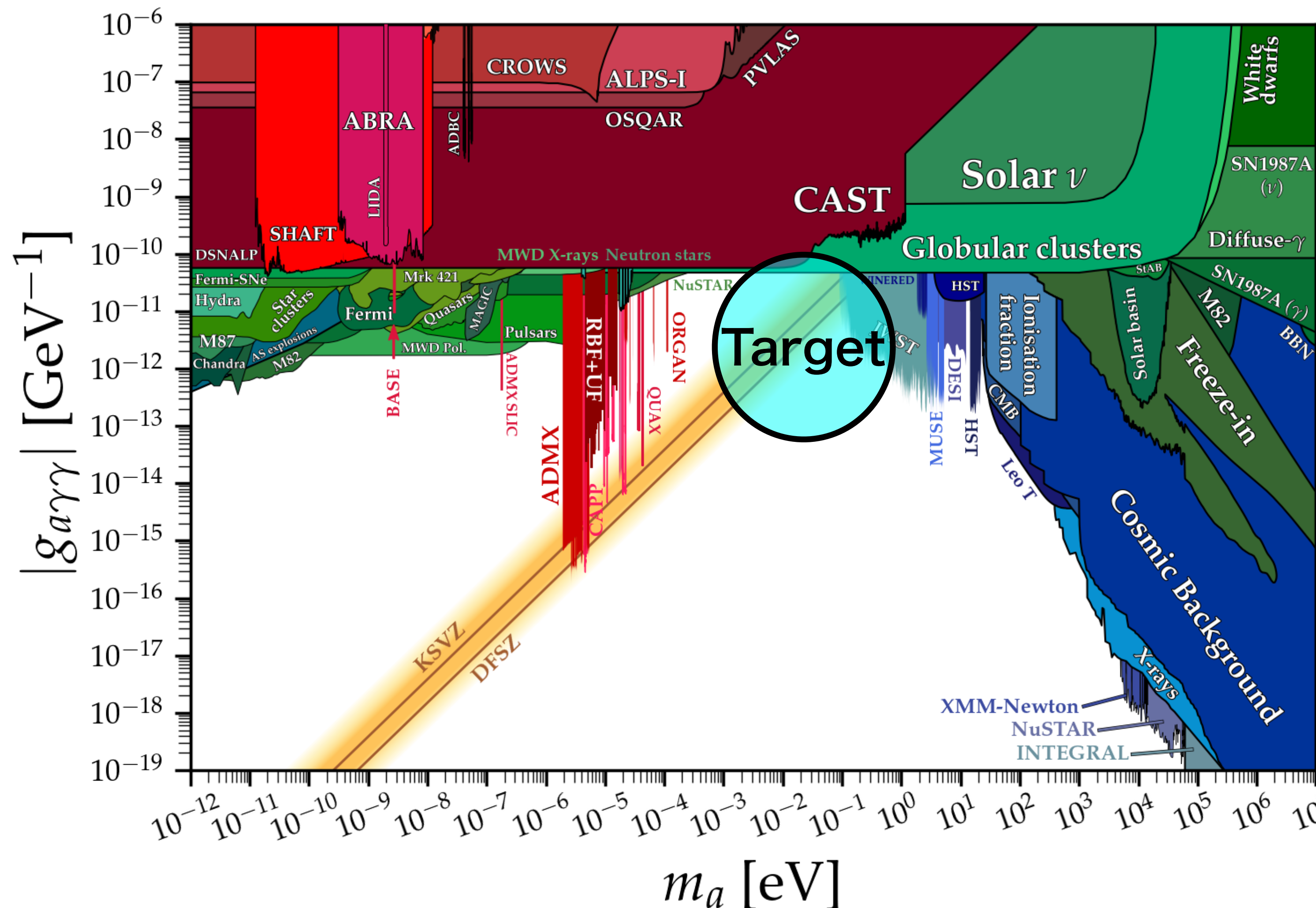
# Shift current is applied in studies of THz dynamics



← Current constraints on

- Axion-photon coupling
- Axion mass

# Shift current is applied in studies of THz dynamics



← Current constraints on

- Axion-photon coupling
- Axion mass

# THz shift current



# meV axion search

# Theoretical form of the shift current

Shift current is regarded as **the second-order DC response**.

The same effect is also observed with **a small output frequency**.

**Theoretical expression for general inputs:**

$$\begin{aligned} \langle \hat{J}_{\text{shift}}^\mu \rangle^{(2)}(\omega) = & \frac{1}{2} \sum_{ab} \int \frac{d^d k}{(2\pi)^d} \int d\omega_1 d\omega_2 \left( \frac{-e^3}{\omega_1 \omega_2} \right) E^{\alpha_1}(\omega_1) E^{\alpha_2}(\omega_2) \delta(\omega - \omega_1 - \omega_2) \\ & \times r_{kab}^{\mu \alpha_1} r_{kba}^{\alpha_2} \left( \frac{f_{ab}}{\omega_2 - \varepsilon_{kba} + i\gamma} \right) + (\alpha_1, \omega_1 \leftrightarrow \alpha_2, \omega_2) \end{aligned}$$

arXiv: 2505.17007

I will pick up some key points.

# Important features for axion search

Output

$$\begin{aligned} \langle \hat{J}_{\text{shift}}^\mu \rangle^{(2)}(\omega) = & \frac{1}{2} \sum_{ab} \int \frac{d^d k}{(2\pi)^d} \int d\omega_1 d\omega_2 \left( \frac{-e^3}{\omega_1 \omega_2} \right) E^{\alpha_1}(\omega_1) E^{\alpha_2}(\omega_2) \delta(\omega - \omega_1 - \omega_2) \\ & \times r_{kab}^{\mu \alpha_1} r_{kba}^{\alpha_2} \left( \frac{f_{ab}}{\omega_2 - \varepsilon_{kba} + i\gamma} \right) + (\alpha_1, \omega_1 \leftrightarrow \alpha_2, \omega_2) \end{aligned}$$

Input

Point!

The second-order response  $\langle \hat{J}^\mu \rangle_{\text{shift}}^{(2)}(\omega) = \sigma_{\text{shift}}^{\mu \alpha_1 \alpha_2} E^{\alpha_1}(\omega_1) E^{\alpha_2}(\omega_2)$

→ We can enhance the signal by applying another strong electric field.

$$J_{\text{shift}}(\omega) = \sigma_{\text{shift}} E_{\text{DM}}(\omega_{\text{DM}}) E_{\text{exp}}(\omega_{\text{exp}}) \quad \sigma_{\text{shift}} : \text{conductivity}$$

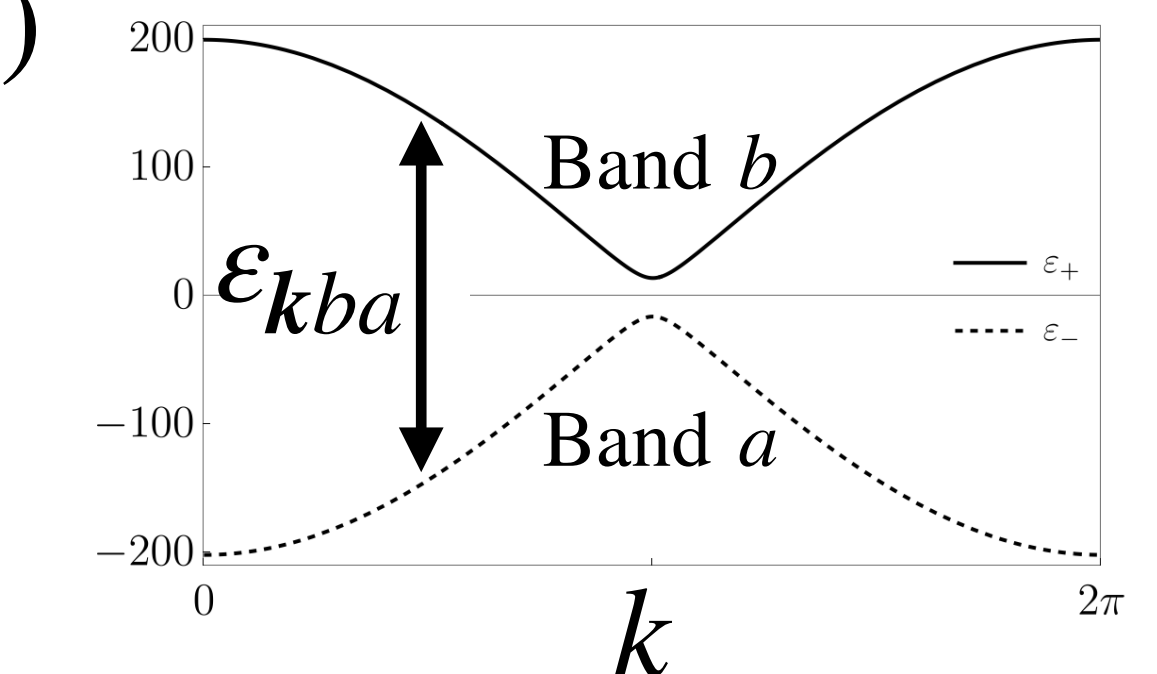
# Important features for axion search

$$\langle \hat{J}_{\text{shift}}^\mu \rangle^{(2)}(\omega) = \frac{1}{2} \sum_{ab} \int \frac{d^d k}{(2\pi)^d} \int d\omega_1 d\omega_2 \left( \frac{-e^3}{\omega_1 \omega_2} \right) E^{\alpha_1}(\omega_1) E^{\alpha_2}(\omega_2) \delta(\omega - \omega_1 - \omega_2)$$

$$\times r_{kab}^{\mu \alpha_1} r_{kba}^{\alpha_2} \left( \frac{f_{ab}}{\omega_2 - \varepsilon_{kba} + i\gamma} \right) + (\alpha_1, \omega_1 \leftrightarrow \alpha_2, \omega_2)$$

Input energy      Band gap of the material

**Point!**



**Band structure restricts the resonant input frequency.**

→ Given the input frequency, the summation and the integration  $\sum_{ab} \int d^d k$  selects the corresponding energy gap  $\varepsilon_{kba}$  to be resonant.

# Important features for axion search

$$\begin{aligned} \langle \hat{J}_{\text{shift}}^\mu \rangle^{(2)}(\omega) = & \frac{1}{2} \sum_{ab} \left[ \frac{d^d k}{(2\pi)^d} \right] d\omega_1 d\omega_2 \left( \frac{-e^3}{\omega_1 \omega_2} \right) E^{\alpha_1}(\omega_1) E^{\alpha_2}(\omega_2) \delta(\omega - \omega_1 - \omega_2) \\ & \times r_{kab}^{\mu \alpha_1} r_{kba}^{\alpha_2} \left( \frac{f_{ab}}{\omega_2 - \varepsilon_{kba} + i\gamma} \right) + (\alpha_1, \omega_1 \leftrightarrow \alpha_2, \omega_2) \end{aligned}$$

**Electron scattering effect**

$$\text{resonant : } \int d^d k \frac{1}{\omega_2 - \varepsilon_{kba} + i\gamma} \sim \gamma \times \frac{1}{i\gamma}$$

**Point!**

**Non-dissipative nature**

$\langle \hat{J}^\mu \rangle_{\text{shift}}^{(2)}(\omega)$  is independent of  $\gamma$

→ This nature, and the wide range of the allowed energy gap supports the broadband search for the axion DM-induced photon.

# I skip the detail of “r”, but…

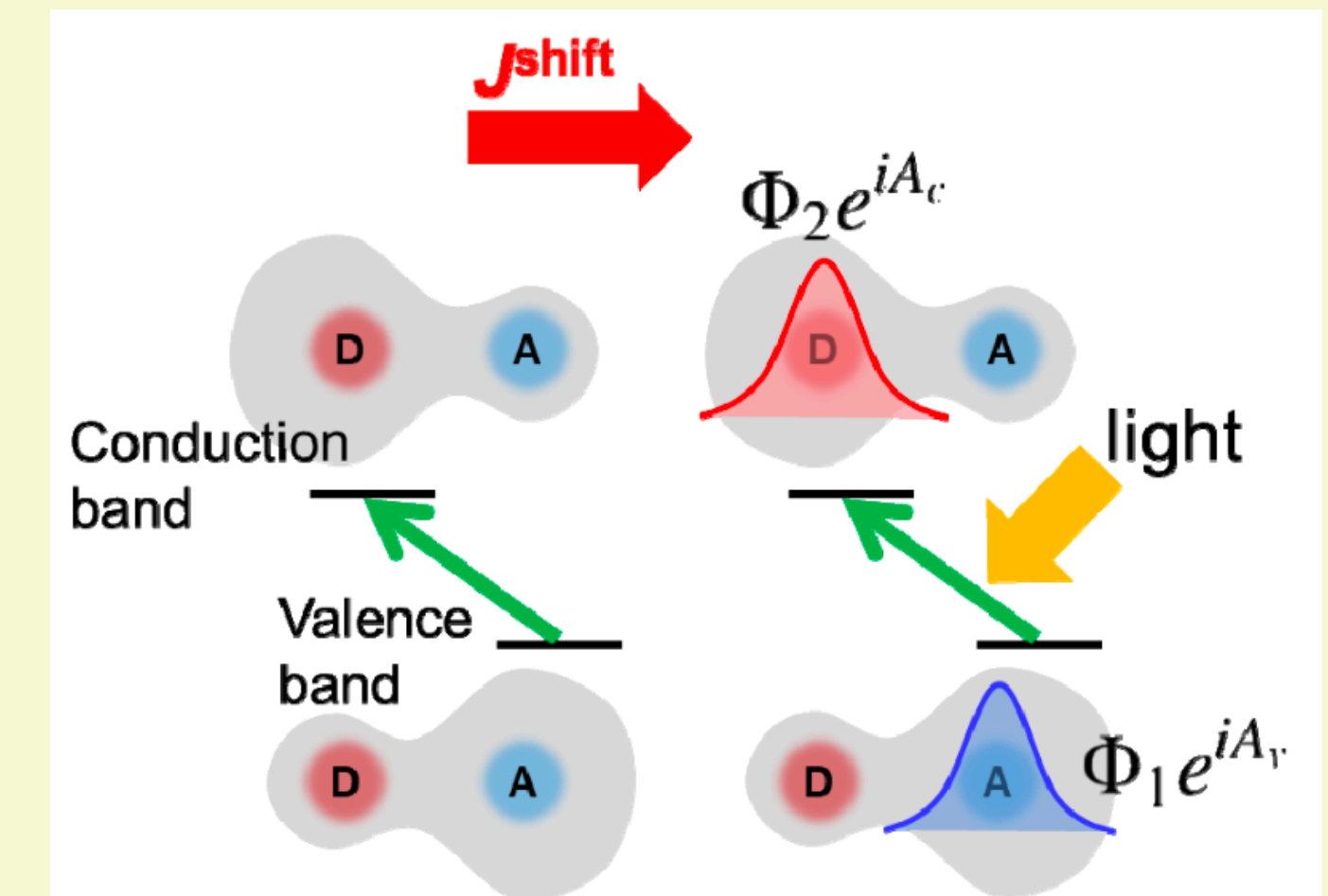
$$\langle \hat{J}_{\text{shift}}^\mu \rangle^{(2)}(\omega) = \frac{1}{2} \sum_{ab} \int \frac{d^d k}{(2\pi)^d} \int d\omega_1 d\omega_2 \left( \frac{-e^3}{\omega_1 \omega_2} \right) E^{\alpha_1}(\omega_1) E^{\alpha_2}(\omega_2) \delta(\omega - \omega_1 - \omega_2)$$

$$\times r_{kab}^{\mu \alpha_1} r_{kba}^{\alpha_2} \left( \frac{f_{ab}}{\omega_2 - \epsilon_{kba} + i\gamma} \right) + (\alpha_1, \omega_1 \leftrightarrow \alpha_2, \omega_2)$$

Contains the information of the Berry connection

## Shift current

- Occurs in the inversion-broken materials.
- It arises from **spatial shift** of the electron wave function during state transitions.



# Outline

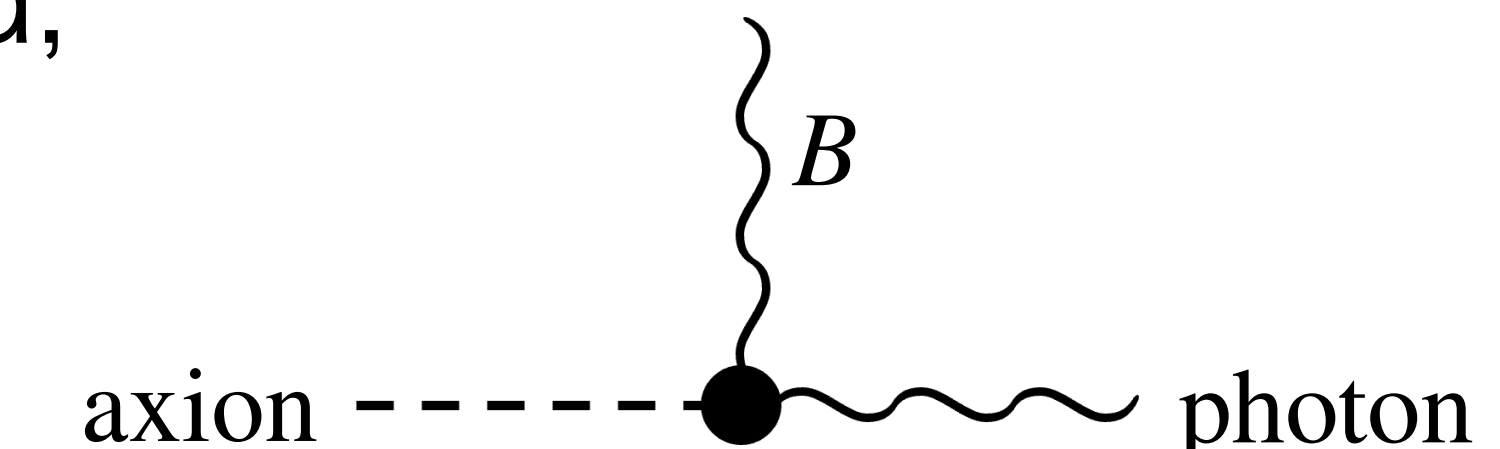
- What is the shift current?
- **Method to detect the axion-induced shift current**

# Step 1: Axion-photon conversion

Interaction:  $\mathcal{L}_{\text{int}} = g_{a\gamma\gamma} a \mathbf{E} \cdot \mathbf{B}$        $a = \frac{\sqrt{2\rho_{\text{DM}}}}{m_{\text{DM}}} \cos(m_{\text{DM}}t + \phi_{\text{DM}})$

In the presence of the static magnetic field,

$$E_{\text{DM}} = g_{a\gamma\gamma} B_0 \frac{\sqrt{2\rho_{\text{DM}}}}{m_{\text{DM}}}$$



$$\simeq 7.9 \times 10^{-12} \frac{\text{V}}{\text{m}} \left( \frac{g_{a\gamma\gamma}}{10^{-11} \text{ GeV}^{-1}} \right) \left( \frac{B_0}{1 \text{ T}} \right) \left( \frac{m_{\text{DM}}}{1 \text{ meV}} \right)^{-1} \left( \frac{\rho_{\text{DM}}}{0.45 \text{ GeV cm}^{-3}} \right)^{\frac{1}{2}}$$

→ Too small to detect directly. (It requires an enhancement mechanism.)

# Step2: Shift current response

**Point!**

**The second-order response**  $\langle \hat{J}^\mu \rangle_{\text{shift}}^{(2)}(\omega) = \sigma_{\text{shift}}^{\mu\alpha_1\alpha_2} E^{\alpha_1}(\omega_1)E^{\alpha_2}(\omega_2)$

→ We can enhance the signal by applying another strong electric field.

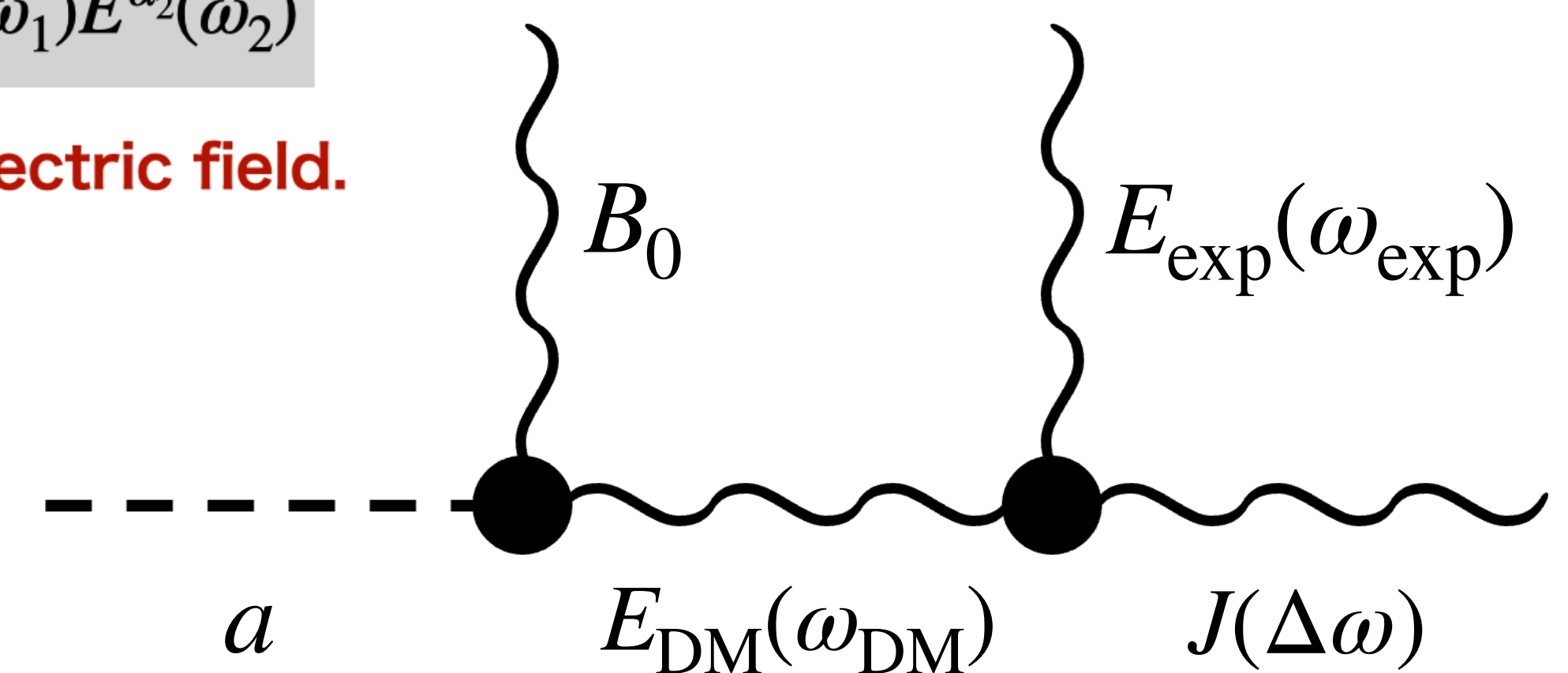
**Input**

$$E(t) = \text{Re} \left[ E_{\text{DM}} e^{im_{\text{DM}}t - i\phi_{\text{DM}}} + E_{\text{exp}} e^{-i\omega_{\text{exp}}t} \right]$$

**Output**

$$\langle \hat{J}^\mu \rangle_{\text{shift}}^{(2)}(\Delta\omega) = \sigma_{\text{shift}}^{\mu\alpha_1\alpha_2}(\Delta\omega) E_{\text{DM}}^{\alpha_1} e^{-i\phi_{\text{DM}}} E_{\text{exp}}^{\alpha_2}$$

$$\Delta\omega = -m_{\text{DM}} + \omega_{\text{exp}}$$

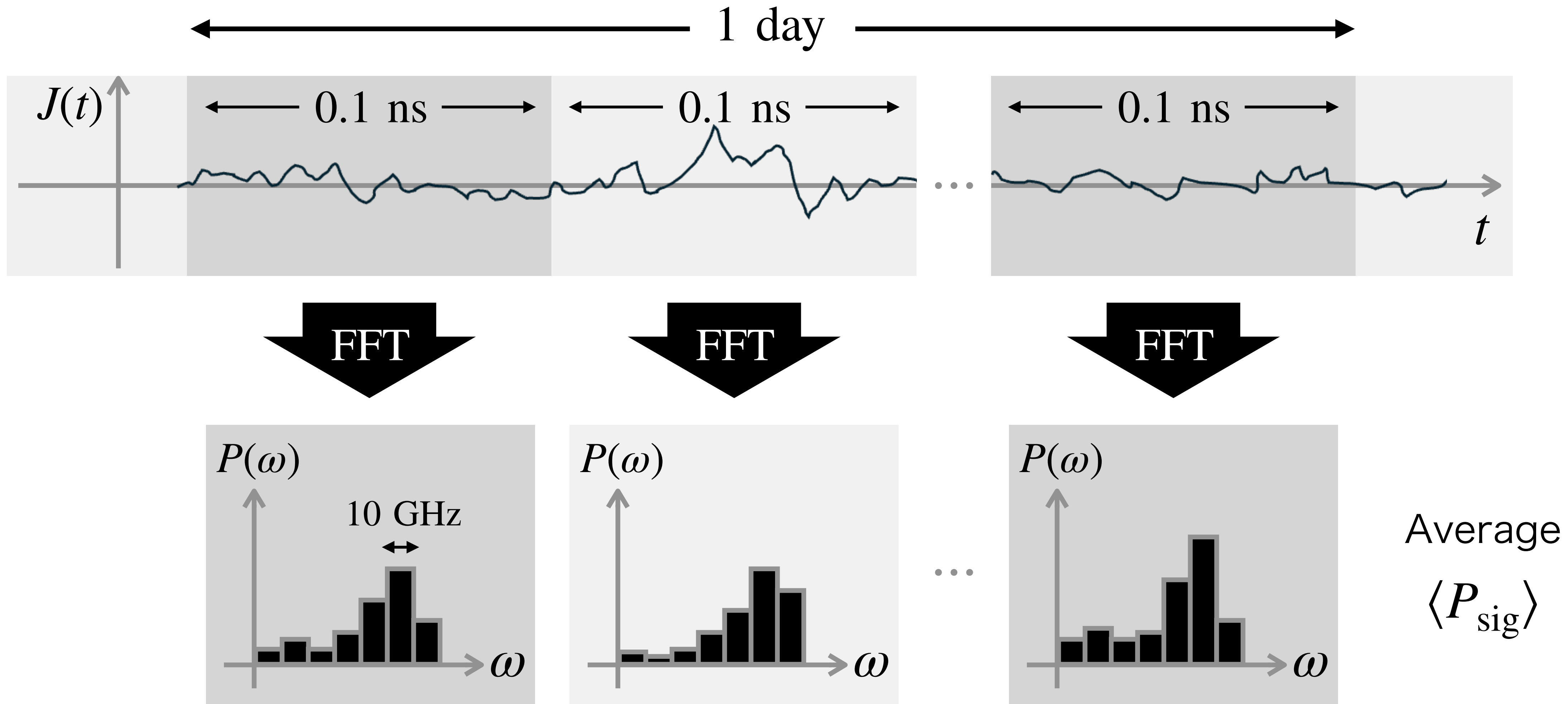


**Other terms**

$J \propto E_{\text{DM}} E_{\text{DM}} \rightarrow \text{Negligible}$

$J \propto E_{\text{exp}} E_{\text{exp}} \rightarrow \text{Background}$

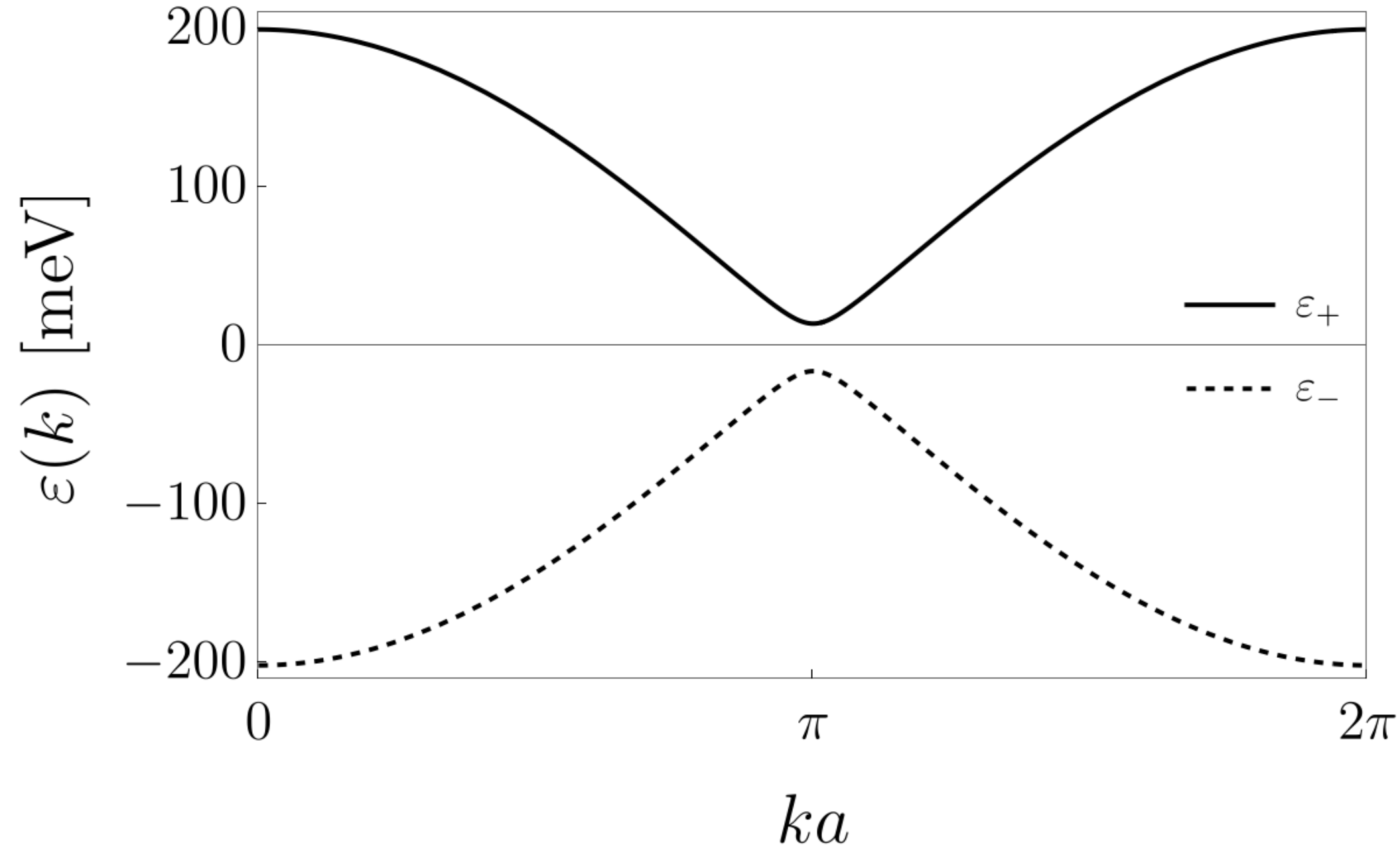
# Step3: Collection of sample data



# Toy model: 1D Rice-mele

$$H(k) = \mathbf{d}(k) \cdot \boldsymbol{\sigma} \quad (\boldsymbol{\sigma} : \text{Pauli matrix})$$

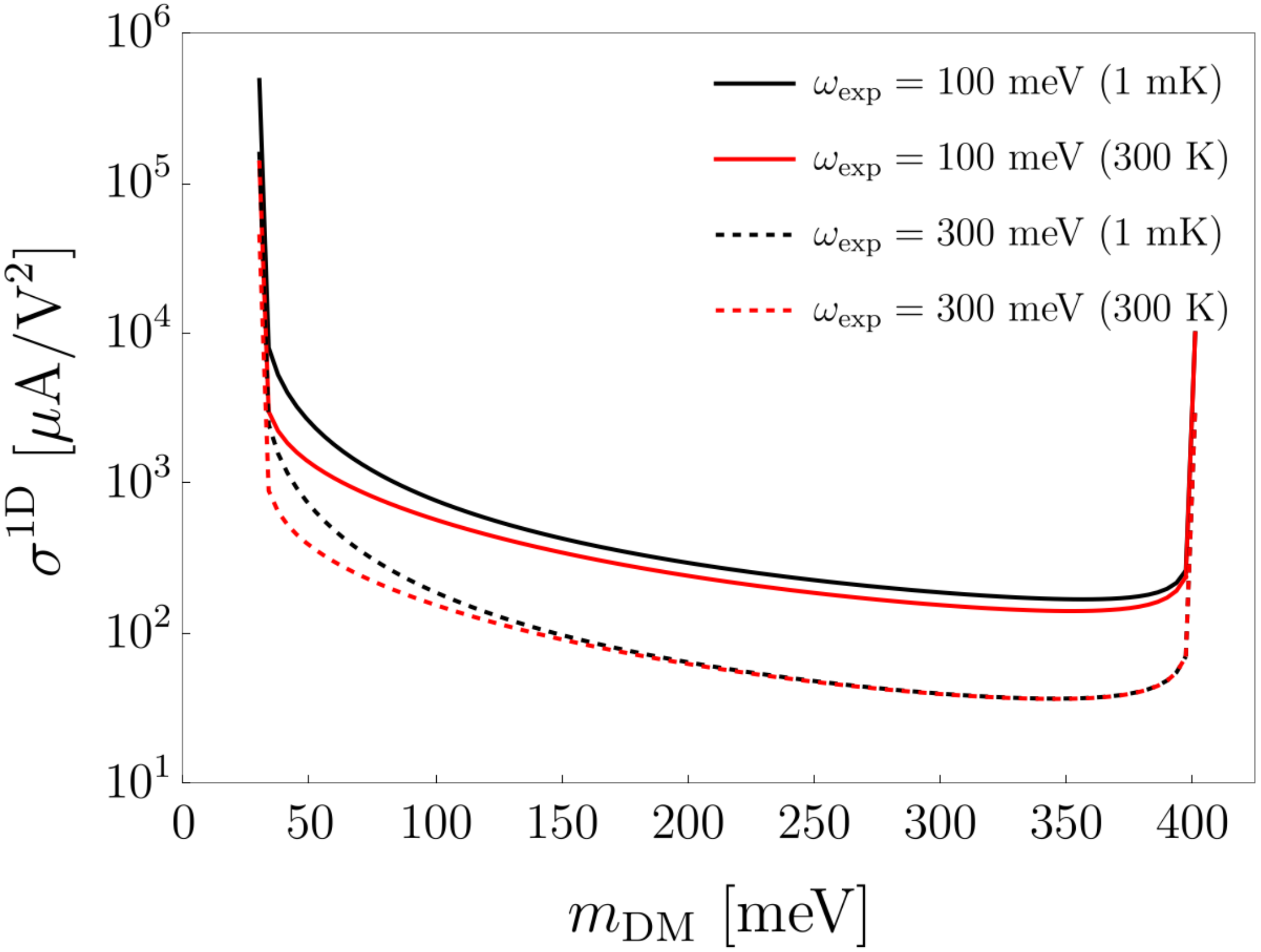
$$d_x = t(1 + \cos ka), \quad d_y = -t \sin ka, \quad d_z = \frac{V_A - V_B}{2}$$



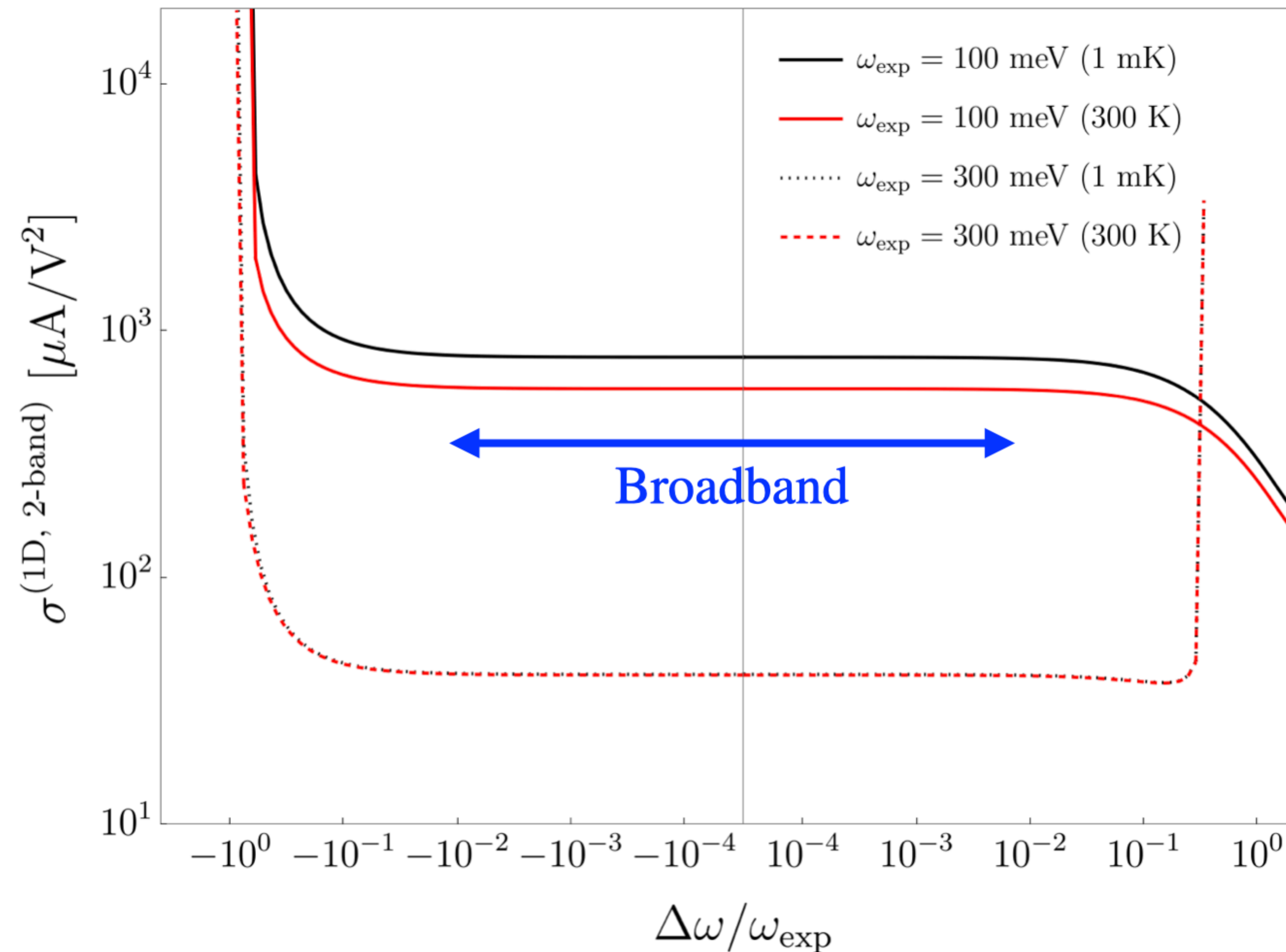
**Point!**

**Band structure determines the resonant input energy.**

→ Sensitive axion mass range is estimated from the band structure.



# Toy model: 1D Rice-mele



The conductivity is almost the same for small  $\Delta\omega$ .

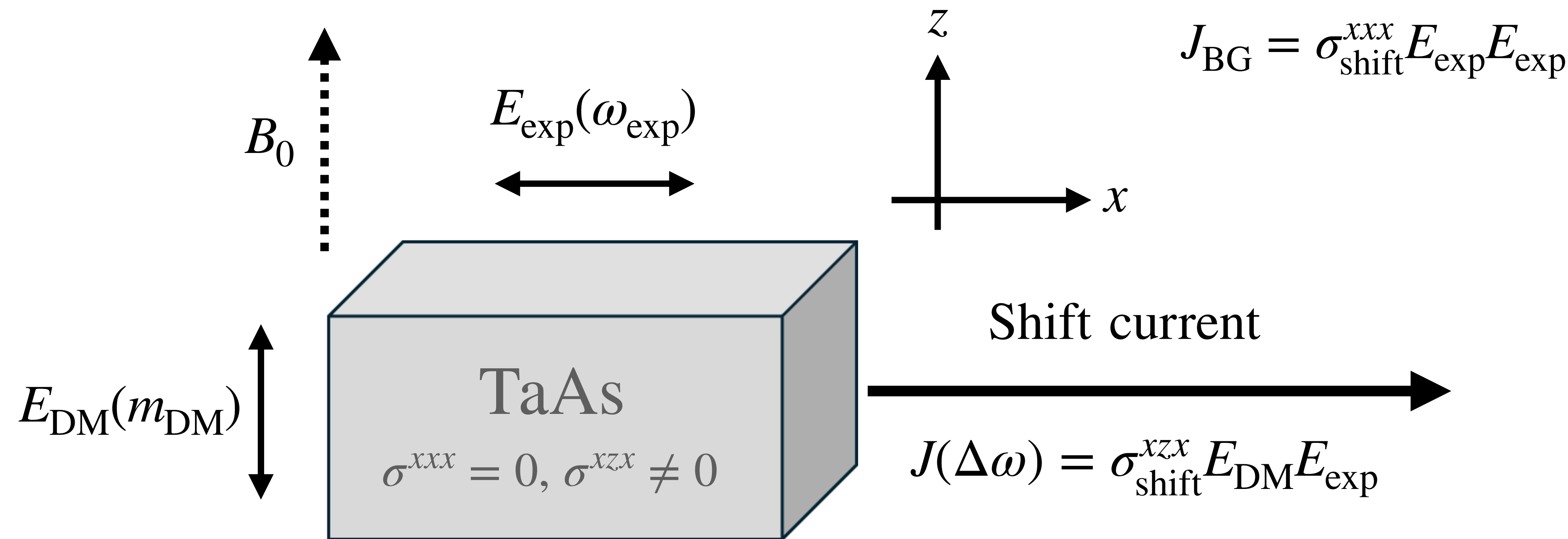
$$\Delta\omega = -m_{\text{DM}} + \omega_{\text{exp}}$$

The search width is not determined by the effect of the electron scattering  $\gamma$ .

**Broadband search is supported!**

# Real material setup

- TaAs: Type-I Weyl semimetal
- $\sigma_{\text{shift}} \sim 200 \mu\text{A}/\text{V}^2$  for  $25 - 350 \text{ meV}$
- Mirror symmetry ( $x \rightarrow -x$ ) is used for cutting backgrounds



# Signal power

$$E(t) = \text{Re} \left[ E_{\text{DM}} e^{im_{\text{DM}}t - i\phi_{\text{DM}}} + E_{\text{exp}} e^{-i\omega_{\text{exp}}t} \right]$$

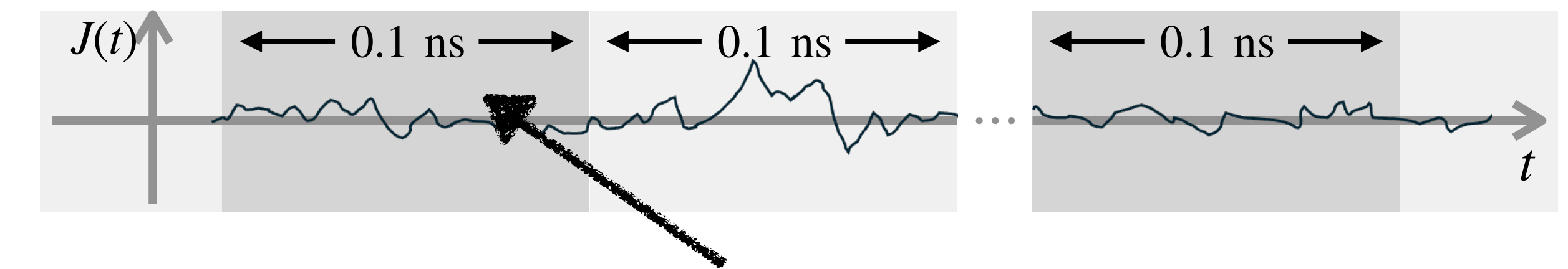
$$\langle \hat{J}^\mu \rangle_{\text{shift}}^{(2)}(\Delta\omega) = \sigma_{\text{shift}}^{\mu\alpha_1\alpha_2}(\Delta\omega) E_{\text{DM}}^{\alpha_1} e^{-i\phi_{\text{DM}}} E_{\text{exp}}^{\alpha_2}$$

$$\Delta\omega = -m_{\text{DM}} + \omega_{\text{exp}}$$

$$\langle P_{\text{sig}} \rangle = \frac{1}{2} R_{\text{exp}} |\sigma_{\text{shift}}^{xzx}|^2 E_{\text{DM}}^2 E_{\text{exp}}^2 L_{\text{exp}}^4$$

$$= 6.2 \times 10^{-15} \mu\text{W} \left( \frac{R_{\text{exp}}}{50 \Omega} \right) \left( \frac{\sigma_{\text{shift}}^{xzx}}{200 \mu\text{A/V}^2} \right)^2 \left( \frac{g_{a\gamma\gamma}}{10^{-11} \text{GeV}^{-1}} \right)^2 \left( \frac{B_0}{1 \text{T}} \right)^2 \\ \times \left( \frac{m_{\text{DM}}}{1 \text{meV}} \right)^{-2} \left( \frac{\rho_{\text{DM}}}{0.45 \text{GeVcm}^{-3}} \right) \left( \frac{E_{\text{exp}}}{10^8 \text{V/m}} \right)^2 \left( \frac{L_{\text{exp}}}{1 \text{cm}} \right)^4$$

We have to take into account the randomness of the unknown relative phase  $\phi_{\text{DM}}$ .



The time interval 0.1 ns is chosen so that it is within the coherent time scale of input fields.

→For each interval, the phase is fixed and we can safely take the average  $\langle P_{\text{sig}} \rangle$ .

# Signal power

$$E(t) = \text{Re} \left[ E_{\text{DM}} e^{im_{\text{DM}}t - i\phi_{\text{DM}}} + E_{\text{exp}} e^{-i\omega_{\text{exp}}t} \right]$$

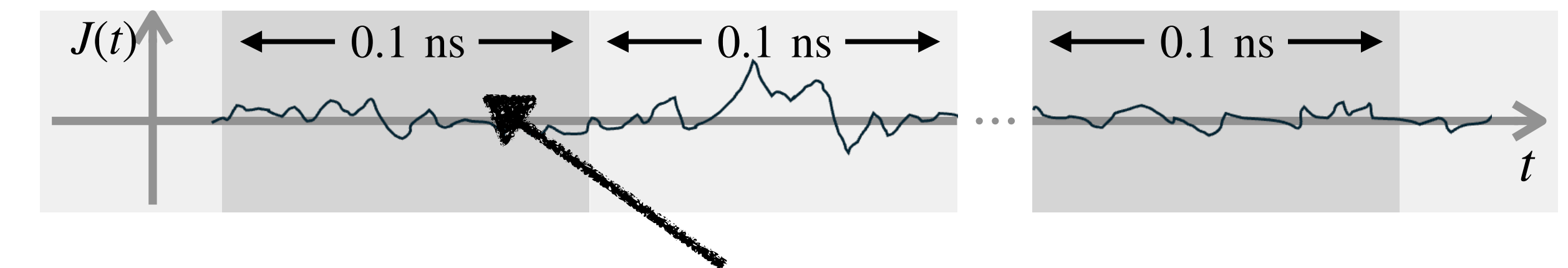
$$\langle \hat{J}^\mu \rangle_{\text{shift}}^{(2)}(\Delta\omega) = \sigma_{\text{shift}}^{\mu\alpha_1\alpha_2}(\Delta\omega) E_{\text{DM}}^{\alpha_1} e^{-i\phi_{\text{DM}}} E_{\text{exp}}^{\alpha_2}$$

$$\Delta\omega = -m_{\text{DM}} + \omega_{\text{exp}}$$

$$\langle P_{\text{sig}} \rangle = \frac{1}{2} R_{\text{exp}} |\sigma_{\text{shift}}^{xzx}|^2 E_{\text{DM}}^2 E_{\text{exp}}^2 L_{\text{exp}}^4$$

$$= 6.2 \times 10^{-15} \mu\text{W} \left( \frac{R_{\text{exp}}}{50 \Omega} \right) \left( \frac{\sigma_{\text{shift}}^{xzx}}{200 \mu\text{A/V}^2} \right)^2 \left( \frac{g_{a\gamma\gamma}}{10^{-11} \text{GeV}^{-1}} \right)^2 \left( \frac{B_0}{1 \text{T}} \right)^2 \\ \times \left( \frac{m_{\text{DM}}}{1 \text{meV}} \right)^{-2} \left( \frac{\rho_{\text{DM}}}{0.45 \text{GeVcm}^{-3}} \right) \left( \frac{E_{\text{exp}}}{10^8 \text{V/m}} \right)^2 \left( \frac{L_{\text{exp}}}{1 \text{cm}} \right)^4$$

We have to take into account the randomness of the unknown relative phase  $\phi_{\text{DM}}$ .



The time interval 0.1 ns is chosen so that it is within the coherent time scale of input fields.

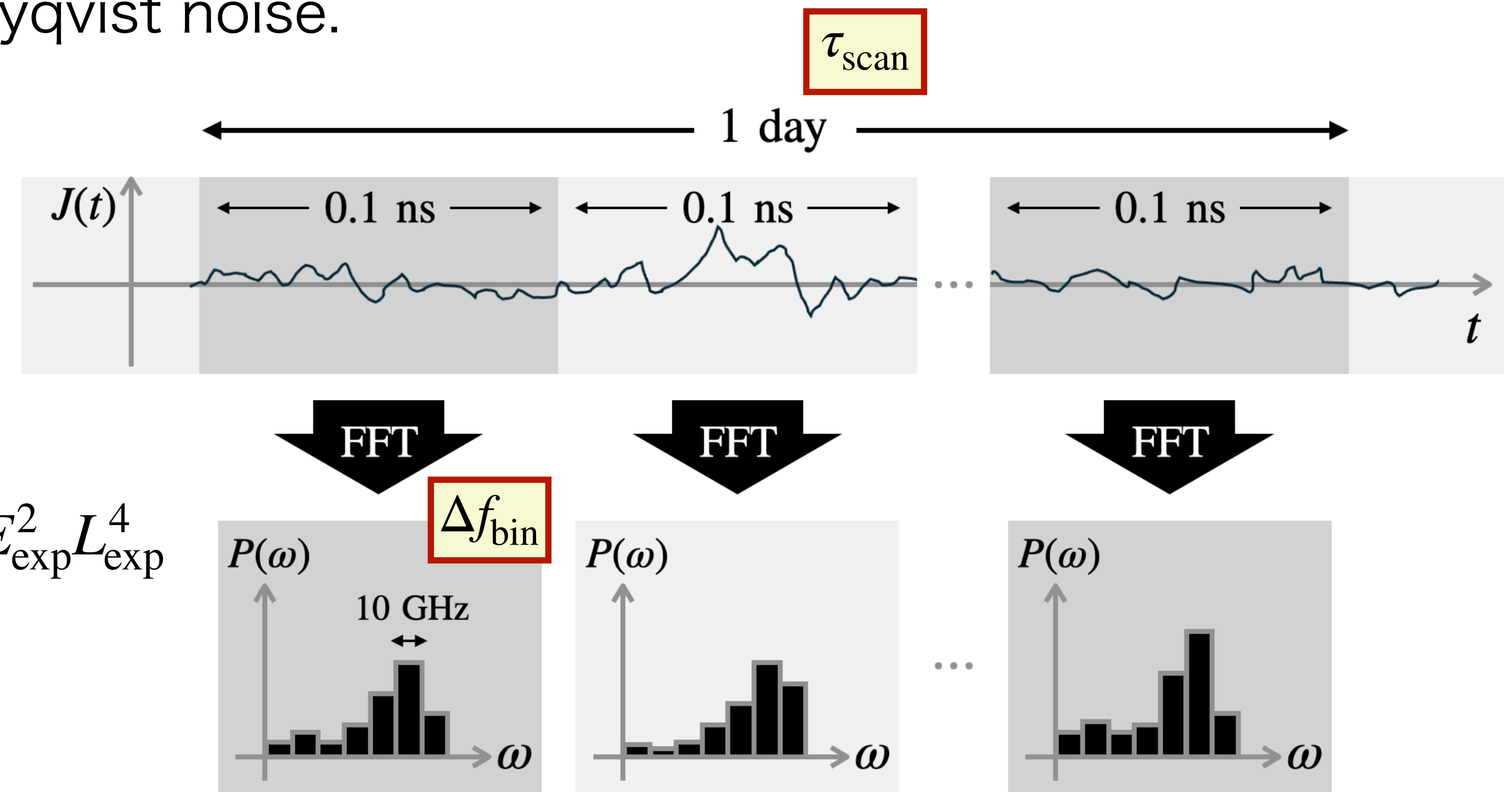
→ For each interval, the phase is fixed and we can safely take the average  $\langle P_{\text{sig}} \rangle$ .

The effect of  $\phi_{\text{DM}}$ .

# Signal to Noise Ratio

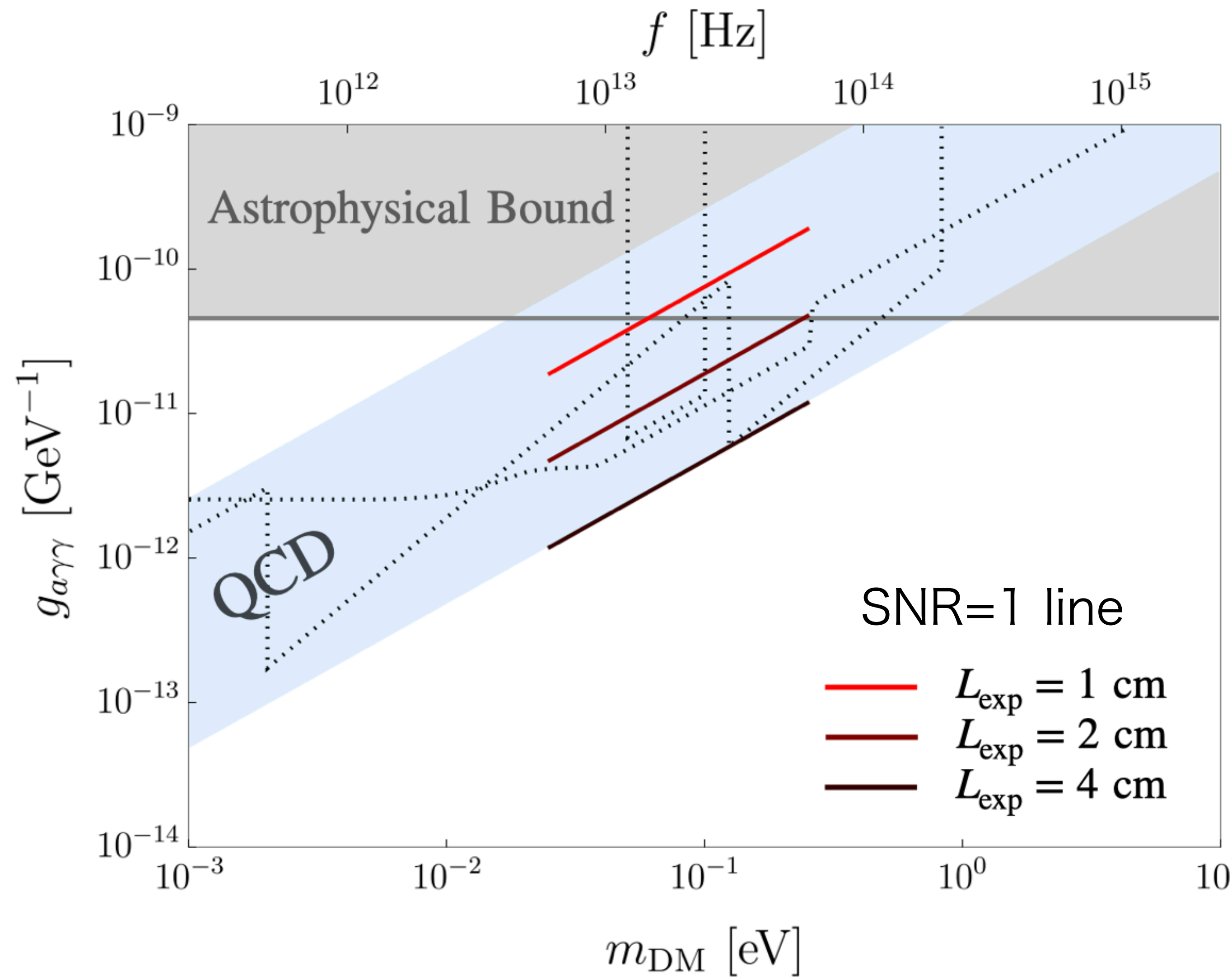
We assume that the main noise comes from Johnson-Nyqvist noise.

$$\text{SNR} = \frac{\langle P_{\text{sig}} \rangle}{4k_B T} \sqrt{\frac{\tau_{\text{scan}}}{\Delta f_{\text{bin}}}}$$



$$\langle P_{\text{sig}} \rangle = \frac{1}{2} R_{\text{exp}} |\sigma_{\text{shift}}^{xzx}|^2 E_{\text{DM}}^2 E_{\text{exp}}^2 L_{\text{exp}}^4$$

# Result

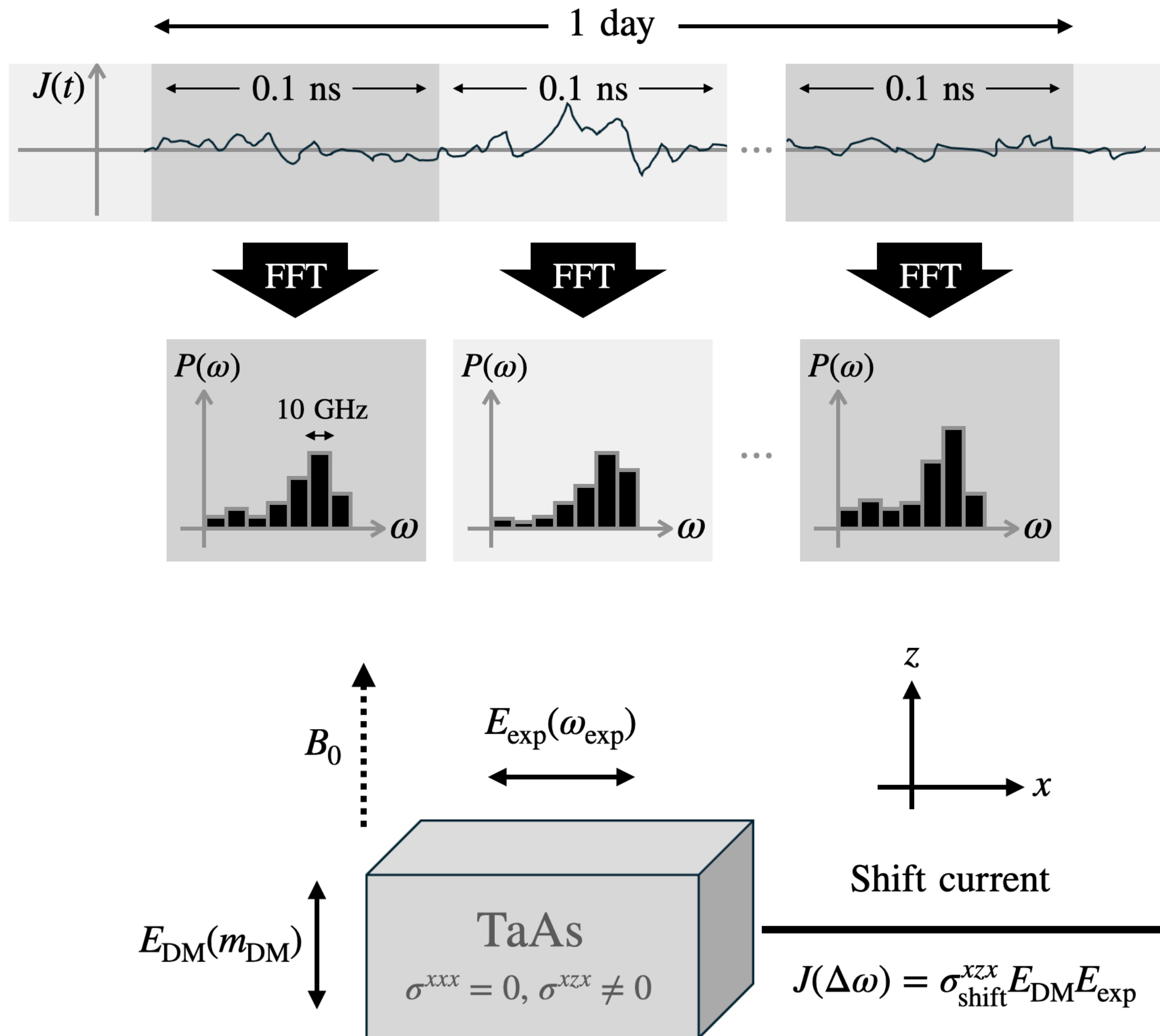


Total mass range:  $25 - 350 \text{ meV}$

Given  $\omega_{\text{exp}} \sim \mathcal{O}(100) \text{ meV}$ ,  
the simultaneous scanning range  
is  $\mathcal{O}(1) \text{ meV}$ .

Spending 1 day for each scan, it  
takes about 300 days to cover  
the whole detectable mass range.

# Some experimental difficulties



① The value of  $E_{\text{exp}} \sim 10^8 \text{ V/m}$  is currently achievable using short-time THz pulse laser technology.  
 $\mathcal{O}(0.1) \text{ ps}$

Y. Sanari, et Al. (2020)

However, our setup requires at least 0.1 ns pulse.

② We excluded the background response by using the symmetry of the material TaAs (Applying the experimental field in x-direction).

But technically, the directional fluctuation of the experimental field cannot be zero. → background

To distinguish the signal from this background, a Gaussian pulse laser must be required.

# Conclusion

We proposed a novel method to detect axion DM using shift current.

Based on our method, it is possible to probe the parameter space of QCD axions in the mass range of  $\mathcal{O}(10) - \mathcal{O}(100)$  meV.

For now, there are several difficulties to realize the experiment ...  
but this is just the beginning of the journey!!

Shift current is the cutting-edge study in condense matter physics.  
(Search for materials with high efficiency, theory, applications, etc.)

→ The development of shift current study helps axion DM search !?.